Modeling, Control and Analysis of a Doubly Fed Induction Generator Based Wind Turbine System: Optimization of the Power Produced

MAROUANE EL AZZAOUI and HASSANE MAHMOUDI
Power electronics and control team,
Department of electrical engineering, Mohammadia School of Engineers,
Mohamed V University Agdal, Rabat, MAROCCO
marouane.elazzaoui@research.emi.ac.ma, mahmoudi@emi.ac.ma

Abstract: - In recent years, wind energy has become one of the most important and promising sources of renewable energy. As a result, wind energy demands additional transmission capacity and better means of maintaining system reliability. The evolution of technology related to the wind system industry has led to the development of a generation of variable speed wind turbines that present numerous advantages compared to fixed-speed wind turbines. This paper deals with the modeling and control of a wind turbine driven doubly fed induction generator (DFIG) that feeds AC power to the utility grid. Initially, a model of the wind turbine and maximum power point tracking (MPPT) control strategy of the doubly-fed induction generator is presented. Thereafter, control vector-oriented stator flux is performed. Finally, the simulation results of the wind system using a doubly-fed of 3MW are presented in a Matlab/Simulink environment.

Key-Words: - Converter, Doubly fed induction generator (DFIG), MPPT, Vector control, Wind turbine.

1 Introduction

Today the production of electrical energy is one of the main causes of air pollution. Produce electricity by continuing to use traditional fossil resources means to pollute the air, water and earth. However, the great opportunity offered by renewable energy can produce electrical energy in a clean way, reducing the incidence of activities and helps to save the environment. Wind power is the one that has the most significant energy potential. The power of the wind turbines installed worldwide increasing more and more every year [1], wind energy systems can no longer behave as only active power generators to distribution or transmission networks, according to the installed power. Indeed, they will certainly be brought in the short term, to provide system services (compensation of reactive power for example) as generators of conventional power plants and / or participate in enhancing the quality of electrical energy (filtering harmonic current in particular).

There are many reasons for using a doubly-fed induction generator for a variable speed wind turbine; such as the accessibility to the stator and rotor provides the opportunity to have more degrees of freedom for well control the transfer of powers [2], has a slightly higher power density than other machines, and increases the speed variation range of ±30% around the synchronous speed, which reduces sizing of the converters between the rotor and the grid.

In this paper, we start with a model of the wind turbine, and present how to maximize the power extracted using MPPT technique, then we make a model of the DFIG in the PARK reference, and the basis of the control of two power converters using vector control, we conclude by presenting in Matlab / Simulink environment the simulation results and their interpretation.

2 wind conversion chain system

The structure used is based on the turbine coupled to the DFIG and the "back to back" converter which is connected between the rotor and the grid (fig.1), allows to pass a fraction of the power through the rotor [3] [4].The performance and power production does not only depend on the DFIG, but also the way in which the two parts of "back-to-back" converter are controlled.

The power converter machine side is called "Rotor Side Converter" (RSC) and the grid side power

converter is called "Grid Side Converter" (GSC). The machine side power converter controls the active power and reactive power produced by the machine. As for the grid-side converter, it controls the DC bus voltage and line-side power factor.

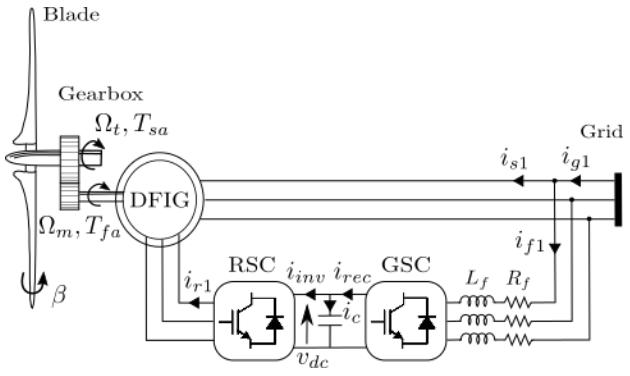

Fig. 1. Structure of a wind energy system based on DFIG

Bernoulli's theorem and the theory of momentum, allow us to express the incident power due to wind [5] [6]:

$$P_{incident} = \frac{1}{2}\rho S v^3 \quad (1)$$

S :the surface swept by the blades of the turbine m^2

ρ :the density of air ($\rho = 1.225 kg/m^3$ at atmospheric pressure)

v : wind speed (m/s)

In a wind energy system, due to various losses, the power extracted from provided on the rotor of the turbine is less than the incident power. The power extracted is expressed by [7].

$$P_{extract} = \frac{1}{2}\rho S C_p(\lambda,\beta) v^3 \quad (2)$$

$C_p(\lambda,\beta)$ is called the power coefficient, which expresses the aerodynamic efficiency of the turbine, it depends on the ratio λ, which is the ratio between the speed at the end of the blades and the wind speed, and the orientation angle β. The ratio λ can be expressed by the following equation [7] [8]:

$$\lambda = \frac{\Omega_t R}{v} \quad (3)$$

Ω_t : The turbine speed of rotation (rad/s).

R : The length of a blade (m).

Albert Betz calculated the maximum of C_p as following [9]:

$$C_{pmax}(\lambda,\beta) = \frac{16}{27} = 0.5926 \quad (4)$$

The model of the power coefficient is given by the following relation [10]:

$$C_{pmax}(\lambda,\beta) = A.sin\left(\frac{\pi(\lambda+0.1)}{14.34-0.3.(\beta-2)}\right) - B \quad (5)$$

With:

$$A = 0.35 - 0.0167.(\beta-2) \quad (6)$$

$$B = 0.00184.(\lambda-3)(\beta-2) \quad (7)$$

Fig.2 shows the evolution of C_p as a function of λ for various β values. This gives a maximum power coefficient of 0.35 for λ equal to 7, maintaining β at $2°$. By setting β and λ to their optimal values, the system will provide optimum electrical power.

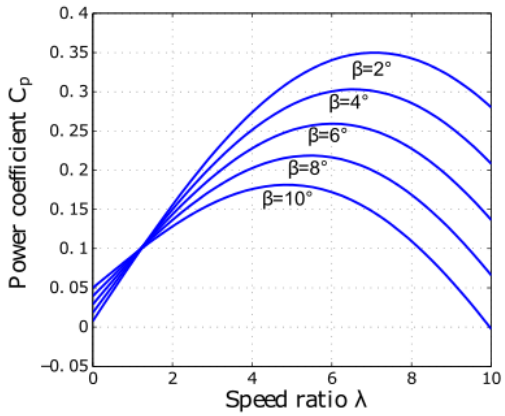

Fig. 2. Power coefficient as a function of speed ratio

Aerodynamic torque on the slow axis is given by [8]:

$$T_{sa} = \frac{1}{2.\Omega_t} C_p(\lambda,\beta)\rho S v^3 \quad (8)$$

The gearbox, which is arranged between the wind turbine and the generator, has aims at adapting the speed of the turbine Ω_t, quite slow, to which the generator requires Ω_m. It is modeled by the following two mathematical equations [7]:

$$\Omega_m = G\Omega_t \tag{9}$$

$$T_{sa} = GT_{fa} \tag{10}$$

The shaft is composed of a mass corresponding to the inertia of the turbine rotor supporting the blades, the hub, and small inertia showing the rotor of the generator. In the proposed mechanical model, the total inertia J is that of the generator J_g and the inertia of turbine J_t applied to the rotor of the generator [8]:

$$J = \frac{J_t}{G^2} + J_g \tag{11}$$

J_t : inertia of the turbine.

J_g : inertia of DFIG.

The evolution of the mechanical speed Ω_m depends on the mechanical torque applied to the generator rotor T_{mec} which is the result of an electromagnetic torque produced by the generator T_{em}, a torque of viscous friction ($f\ \Omega_m$) and a torque in fast axis T_{fa}, as follows [11]:

$$J\frac{d\Omega_m}{dt} = T_{mec} = T_{fa} - T_{em} - f\Omega_m \tag{12}$$

The previous relations used to establish the block diagram of the mechanical part of the wind system (fig.3).

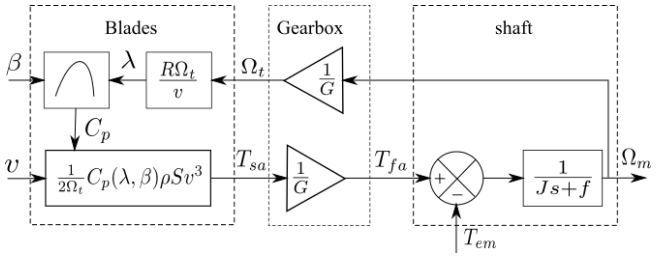

Fig. 3. Block diagram of the turbine model

3 Maximum power extraction

In practice, an accurate measurement of wind speed is sometimes hard to get, leading to a degradation of the received power. This is why most wind turbines are controlled without control of the speed [12].

This control structure is based on the assumption that the wind speed varies very little steady. In this case, from the dynamic equation of the turbine, we obtain the static equation describing the standing turbine speed:

$$J\frac{d\Omega_m}{dt} = 0 = T_{mec} = T_{fa} - T_{em} - f\Omega_m \tag{13}$$

This means considering the mechanical torque developed at zero, we obtain:

$$T_{em} = T_{fa} - f\Omega_m \tag{14}$$

The controller in this case sh ould impose reference torque to allow DFIG turning at an adjustable speed to ensure optimal operating point of power extraction. In this context, the ratio of the speed of wind λ must be maintained at its optimum value ($\lambda = \lambda_{opt}$) on a certain wind speed range. Thus, the power coefficient would be kept at its maximum value ($C_p = C_{pmax}$).The aerodynamic torque on t he slow axis will in this case as an expression:

$$T_{sa} = \frac{1}{2.\Omega_t} C_{pmax}\rho Sv^3 \tag{15}$$

At the output of the gearbox, reference torque becomes:

$$T_{em}^* = T_{fa}^* - f\Omega_m = \frac{1}{G}T_{sa} - f\Omega_m \tag{16}$$

Substituting the expression of T_{sa} , we get:

$$T_{em}^* = \frac{1}{2G\Omega_t} C_{pmax}\rho Sv^3 - f\Omega_m \tag{17}$$

An estimate of the speed of the turbine Ω_t is calculated from equation (9):

$$\Omega_t = \frac{1}{G}\Omega_m \tag{18}$$

Assuming that the orientation angle β of the blades is constant, the wind speed can be estimated from equation (3) as follows:

$$v = \frac{R\Omega_t}{\lambda_{opt}} \tag{19}$$

The electromagnetic torque reference will be expressed as:

$$T_{em}^{*} = \frac{1}{2G^3\lambda_{opt}^3} C_{pmax}\rho\pi R^5\Omega_m^2 - f\Omega_m \quad (20)$$

The representation of a block diagram is shown in fig.4.

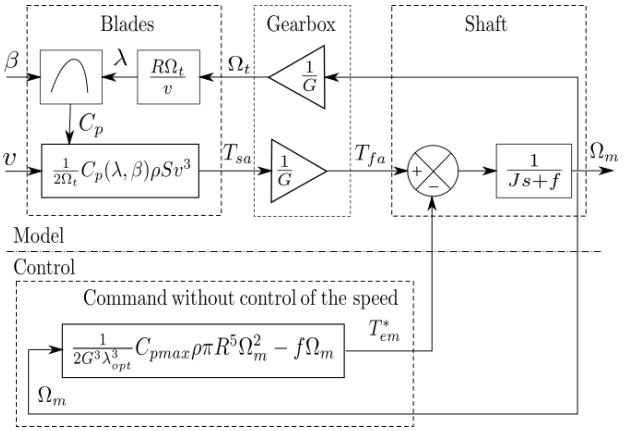

Fig. 4. Block diagram without control of the speed

4 Modeling of DFIG

The electrical equations of DFIG in the (dq) reference can be written [8] [13]:

$$v_{sd} = R_s i_{sd} + \frac{d\phi_{sd}}{dt} - \omega_s\phi_{sq} \quad (21)$$

$$v_{sq} = R_s i_{sq} + \frac{d\phi_{sq}}{dt} + \omega_s\phi_{sd} \quad (22)$$

$$v_{rd} = R_r i_{rd} + \frac{d\phi_{rd}}{dt} - \omega_r\phi_{rq} \quad (23)$$

$$v_{rq} = R_r i_{rq} + \frac{d\phi_{rq}}{dt} + \omega_r\phi_{rd} \quad (24)$$

The pulse of the stator currents being constant, the rotor pulse is derived from [8] [13]:

$$\omega_r = \omega_s - p\Omega_m \quad (25)$$

The equations for the flux in (dq) reference are given by [8] [13]:

$$\phi_{sd} = L_s i_{sd} + M i_{rd} \quad (26)$$

$$\phi_{sq} = L_s i_{sq} + M i_{rq} \quad (27)$$

$$\phi_{rd} = L_r i_{rd} + M i_{sd} \quad (28)$$

$$\phi_{rq} = L_r i_{rq} + M i_{sq} \quad (29)$$

With:

$L_s = l_s - M_s$: Cyclic inductance of stator phase.

$L_r = l_r - M_r$: Cyclic inductance of rotor phase.

l_s and l_r : inductors own stator and rotor of the machine.

M_s and M_r : mutual inductances between two stator phases and between two rotor phases of the machine.

M : maximum mutual inductance between stator and rotor stage

p : number of pairs of poles of the DFIG.

The electromagnetic torque is expressed by [8]:

$$T_{em} = p(\phi_{sd} i_{sq} - \phi_{sq} i_{sd}) \quad (30)$$

The active and reactive power of the stator and rotor are written as follows [8] [13]:

$$P_s = v_{sd} i_{sd} + v_{sq} i_{sq} \quad (31)$$

$$Q_s = v_{sq} i_{sd} - v_{sd} i_{sq} \quad (32)$$

$$P_r = v_{rd} i_{rd} - v_{rq} i_{rq} \quad (33)$$

$$Q_r = v_{rq} i_{rd} - v_{rd} i_{rq} \quad (34)$$

5 Vector control of DFIG

DFIG control strategies are based on two different approaches [14]:

- Flow control in closed loop, where the frequency and voltage are considered variables (unstable grid).
- Flow control in open loop when the voltage and frequency are constant (stable grid).

In our study, the frequency and voltage are deemed to be unchanging. We can be clear from equation (30), the strong coupling between flows and currents. Indeed, the electromagnetic torque is the cross product between flows and stator currents, making the control of DFIG particularly difficult. To simplify ordering, we approximate the model to that of the DC machine which has the merit of having a natural coupling between flows and currents. For this, we apply vector control, also

known order by the direction of flow. We choose (dq) reference linked to the rotating field (fig. 5) [15].

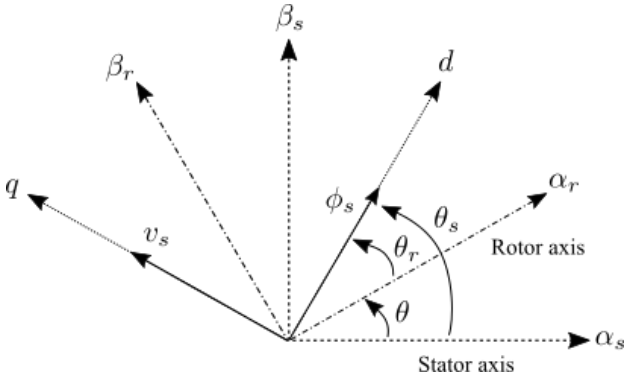

Fig. 5. Orientation of the axis d to stator flux

Fig.5 shows that the stator flux ϕ_s coincides with the axis (d), which allows writing [15]:

$$\phi_{sd} = \phi_s \tag{35}$$

$$\phi_{sq} = 0 \tag{36}$$

From equations (26) and (27), we can write:

$$\phi_{sd} = L_s i_{sd} + M i_{rd} = \phi_s \tag{37}$$

$$\phi_{sq} = L_s i_{sq} + M i_{rq} = 0 \tag{38}$$

In the field of production of wind energy, these are average machines and high power which are mainly used. Thus, we neglect the stator resistance. Taking the constant stator flux, we can write:

$$v_{sd} = 0 \tag{39}$$

$$v_{sq} = V_s = \omega_s \phi_s \tag{40}$$

To determine the angles necessary for transformation Park of the stator variables (θ_s) and the rotor variables (θ_r), we used a phase locked loop (PLL) as showed in fig.6. This PLL allows to accurately estimate the frequency and amplitude of the grid [16].

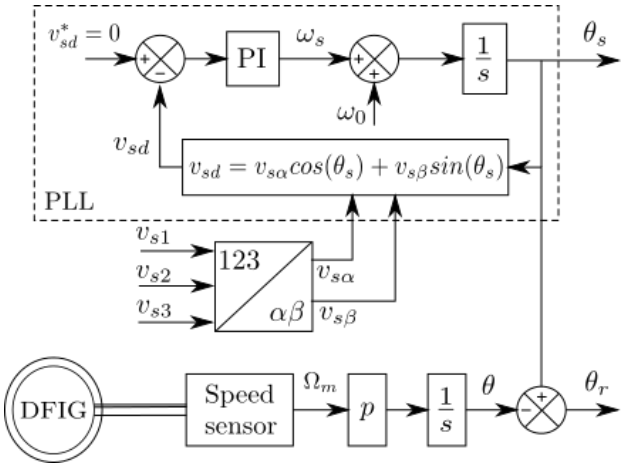

Fig. 6. Establishment angles processing using a PLL

The architecture of the controller is illustrated in fig.7. It is built on the three-phase model of the electromechanical conversion chain of the wind energy system [17].

Three commands are needed:

- Maximum extraction control wind power by controlling said MPPT (detailed in Section III).
- Control of RSC by controlling the electromagnetic torque and stator reactive power of DFIG
- Control of GSC by controlling the voltage of the DC bus and the active and reactive power exchanged with the grid.

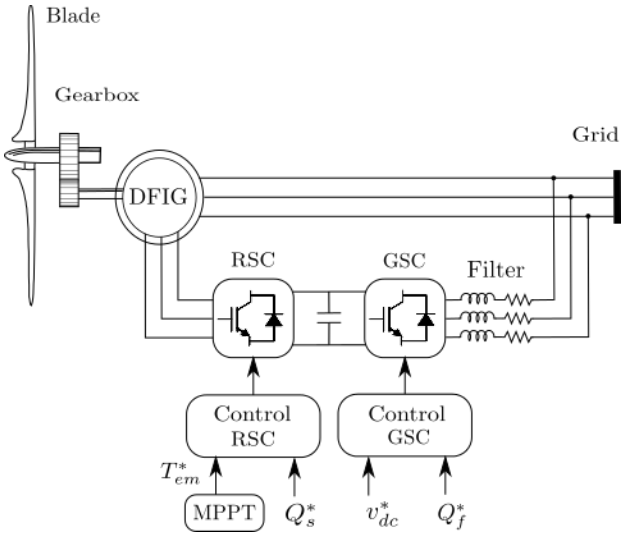

Fig. 7. Control architecture of the wind system

5.1 Control of the rotor side converter

The principle of the control of the rotor side converter is shown in fig.8 [17].

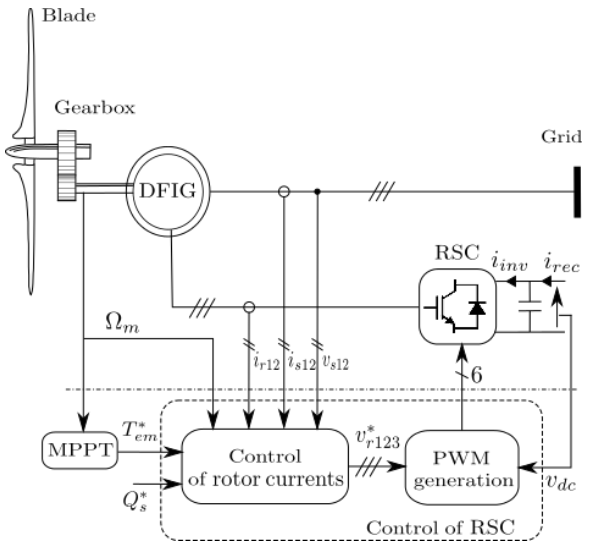

Fig. 8. Principle of the Control of the rotor side converter

The controls of electromagnetic torque and stator reactive power will be obtained by controlling the rotor (dq) axes currents of DFIG. From the equations (37) to (40) we obtain the expression of the stator current:

$$i_{sd} = \frac{v_{sq}}{\omega_s L_s} - \frac{M}{L_s} i_{rd} \tag{41}$$

$$i_{sq} = -\frac{M}{L_s} i_{rq} \tag{42}$$

These expressions are then substituted in the equations (28) and (29) of the rotor flux which then becomes:

$$\phi_{rd} = \sigma L_r i_{rd} + \frac{M v_{sq}}{\omega_s L_s} \tag{43}$$

$$\phi_{rq} = \sigma L_r i_{rq} \tag{44}$$

With:

$\sigma = 1 - \frac{M^2}{L_r L_s}$: the dispersion coefficient of the DFIG.

Substituting the expressions of the direct and quadrature components of the rotor flux in the equations (23) and (24) we get:

$$v_{rd} = R_r i_{rd} + \sigma L_r \frac{di_{rd}}{dt} + e_{rd} \tag{45}$$

$$v_{rq} = R_r i_{rq} + \sigma L_r \frac{di_{rq}}{dt} + e_{rq} + e_{\phi} \tag{46}$$

With:

$$e_{rd} = -\sigma L_r \omega_r i_{rq} \tag{47}$$

$$e_{rq} = \sigma L_r \omega_r i_{rd} \tag{48}$$

$$e_{\phi} = \frac{\omega_r M v_{sq}}{\omega_s L_s} \tag{49}$$

Replacing the expressions of i_{sd}, i_{sq} and ϕ_{sd} in the expression of the electromagnetic torque in equation (30) we get:

$$T_{em} = -\frac{pMv_{sq}}{\omega_s L_s} i_{rq} \tag{50}$$

Substituting the expressions of i_{sd}, i_{sq} in equations (31) and (32), we get the expressions of stator active and reactive powers :

$$P_s = -v_{sq} \frac{M}{L_s} i_{rq} \tag{51}$$

$$Q_s = \frac{v_{sq}^2}{\omega_s L_s} - \frac{M v_{sq}}{L_s} i_{rd} \tag{52}$$

These last expressions show that the choice of coordinate system (dq) makes the electromagnetic torque produced by the DFIG, and therefore the stator power, proportional to the current of the rotor axis (q). The stator reactive power, in turn, is proportional to the current of the rotor axis (d) due to a constant imposed by the grid. Thus, these stator powers can be controlled independently of one another. This shows us that we can set up a control rotor current due to the influence of the couplings. Every current can be controlled independently each with its own controller. The reference values for these regulators will be the rotor axis current (q) and the rotor axis current (d) .The block diagram of the control loops of the axis rotor currents (dq) is shown in fig.9, regulators used are PI correctors.

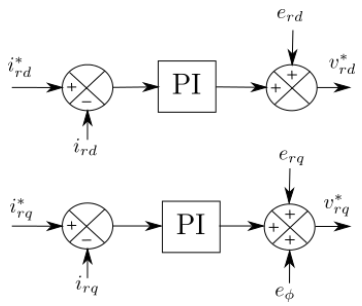

Fig. 9. Control of rotor currents

The rotor current of the reference axis (q) is derived from the MPPT control via the electromagnetic torque reference (fig.4). The rotor current of the reference axis (d) is derived from the control of the stator reactive power.

From the equations (50) and (52) we obtain:

$$i_{rd}^{*} = -\frac{L_s}{Mv_{sq}}Q_s^{*} + \frac{v_{sq}}{\omega_s M} \tag{53}$$

$$i_{rq}^{*} = -\frac{\omega_s L_s}{pMv_{sq}}T_{em}^{*} \tag{54}$$

Fig.10 shows the block diagram of the control of RSC.

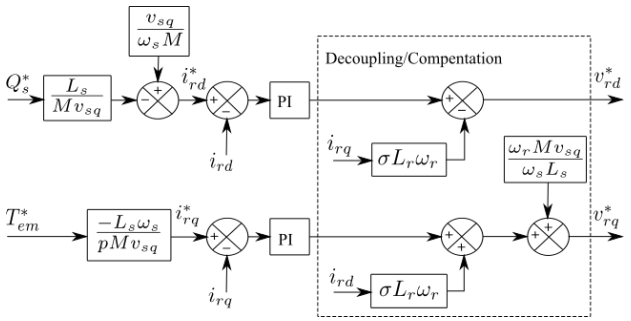

Fig. 10. Control of rotor side converter

5.2 Control of the grid side converter

Fig.11 shows the principle of the control of the rotor side converter performs the following two functions [17]:

- Control currents that flowing in the RL filter.
- Control voltage of the DC bus.

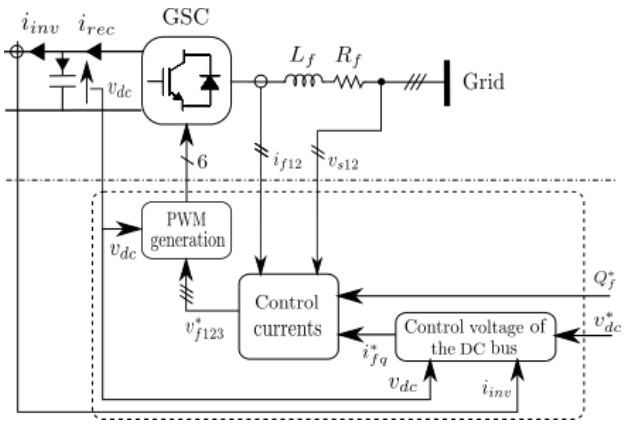

Fig. 11. Principle of the control of the grid side converter

5.2.1 Control currents flowing in the RL filter

According to Kirchhoff's laws, the equations of the filter in the three-phase reference voltages are given by [17]:

$$v_{f1} = -R_f i_{f1} - L_f \frac{di_{f1}}{dt} + v_{s1} \tag{55}$$

$$v_{f2} = -R_f i_{f2} - L_f \frac{di_{f2}}{dt} + v_{s2} \tag{56}$$

$$v_{f3} = -R_f i_{f3} - L_f \frac{di_{f3}}{dt} + v_{s3} \tag{57}$$

Applying the Park transformation, we obtain:

$$v_{fd} = -R_f i_{fd} - L_f \frac{di_{fd}}{dt} + e_{fd} \tag{58}$$

$$v_{fq} = -R_f i_{fq} - L_f \frac{di_{fq}}{dt} + e_{fq} \tag{59}$$

With:

$$e_{fd} = \omega_s L_f i_{fq} \tag{60}$$

$$e_{fq} = -\omega_s L_f i_{fd} + v_{sq} \tag{61}$$

The pattern of binding of GSC to grid in the landmark Park along the stator rotating field shows us that we can put in place a control of the currents flowing in the RL filter is given to the influence of the couplings, every axis can be controlled independently with each its own PI controller. The reference values for these controllers will be the current in RL filter (fig.12).

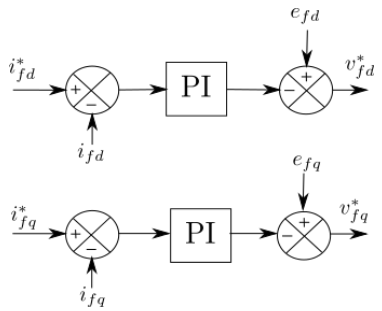

Fig. 12. Control currents flowing in the RL filter

Reference currents i^*_{fd} and i^*_{fq} are respectively given from the control block of the DC bus and control of reactive power at the GSC connection point to the grid (fig.11).

Neglecting losses in R_f resistance of RL filter and taking the orientation of the coordinate system (dq) connected to the rotary stator field ($v_{sd} = 0$), the equations for the powers generated by the GSC are given by [17]:

$$P_f = v_{sq} i_{fq} \tag{62}$$

$$Q_f = v_{sq} i_{fd} \tag{63}$$

From these equations, it is possible to impose the active and reactive power reference noted here P^*_f and Q^*_f, imposing the following reference currents:

$$i^*_{fd} = \frac{Q^*_f}{v_{sq}} \tag{64}$$

$$i^*_{fq} = \frac{P^*_f}{v_{sq}} \tag{65}$$

5.2.2 Control of the DC bus voltage

We can express of the powers involved on the DC bus by [17]:

$$P_{rec} = v_{dc} i_{rec} \tag{66}$$

$$P_c = v_{dc} i_c \tag{67}$$

$$P_{inv} = v_{dc} i_{inv} \tag{68}$$

These powers are linked by the relation [17]:

$$P_{rec} = P_c + P_{inv} \tag{69}$$

Neglecting all the Joule losses (losses in the capacitor, the converter and the RL filter), we can write:

$$P_f = P_{rec} = P_c + P_{inv} \tag{70}$$

By adjusting the power P_f , then it is possible to control the power P_c in the capacitor and therefore to regulate the DC bus voltage. To do this, the P_{inv} and P_c powers must be known to determine P^*_f. The reference power for the capacitor is connected to the reference current flowing through the capacitor:

$$P^*_c = v_{dc} i^*_c \tag{71}$$

Fig.13 shows that we can regulate the DC bus voltage using an external loop, based on a PI controller that generates the reference i^*_c.

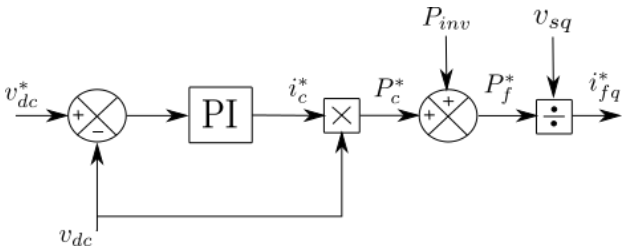

Fig. 13. Control loop of the DC bus voltage

Fig.14 shows the block diagram of the control of GSC. This block diagram includes the terms of decoupling and compensation to be able to independently control the (dq) axes currents circulating in the RL filter and the active and reactive power exchanged between the GSC and the grid.

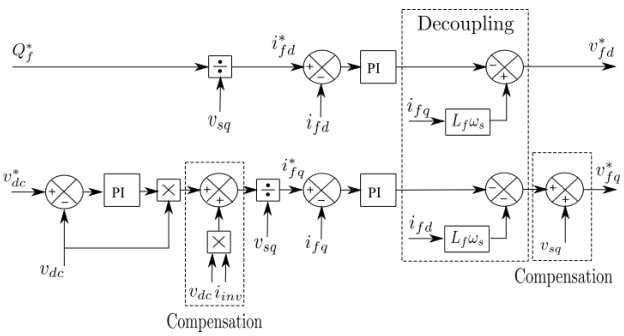

Fig. 14. Control of grid side converter

6 Simulation Results

The simulations of the whole system were performed with Matlab / Simulink, the DC bus reference voltage, denoted v_{dc}^{*} is set at 1200 V. The reactive power reference Q_f^{*} is set to 0 VAr, which guarantees a unitary power factor at the GSC connection to the grid. By cons, we will vary the stator reactive power Q_s by adjusting the reference value in the RSC control. We present in this section the results of the proposed control.

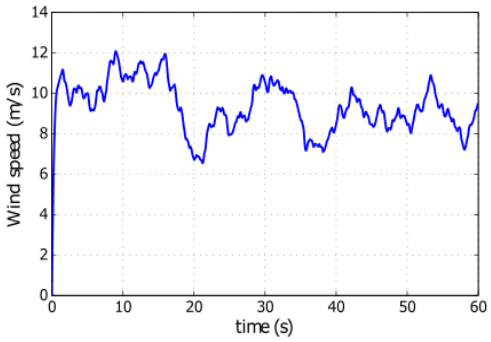

Fig. 15. Wind speed

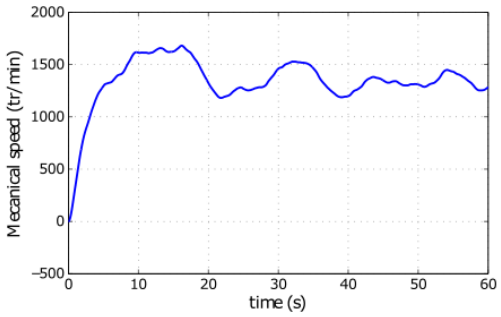

Fig. 16. Mechanical speed

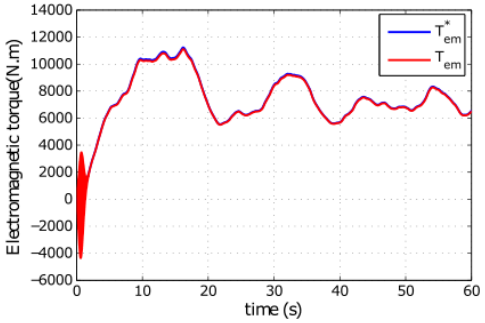

Fig. 17. Electromagnetic torque (reference and simulated)

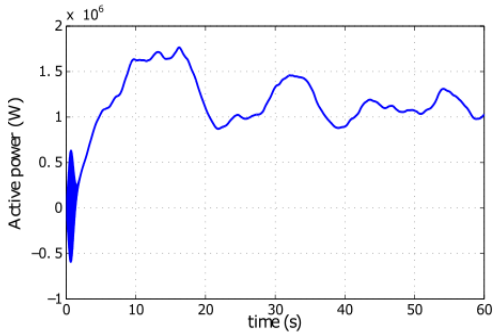

Fig. 18. Stator active power

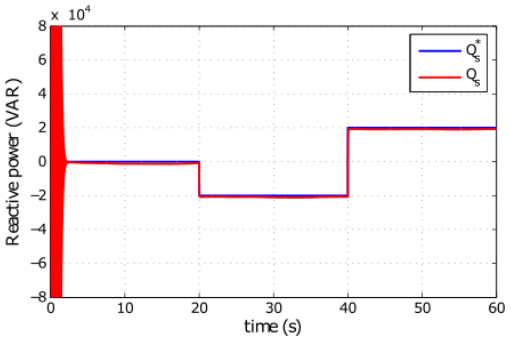

Fig. 19. Stator reactive power (reference and simulated)

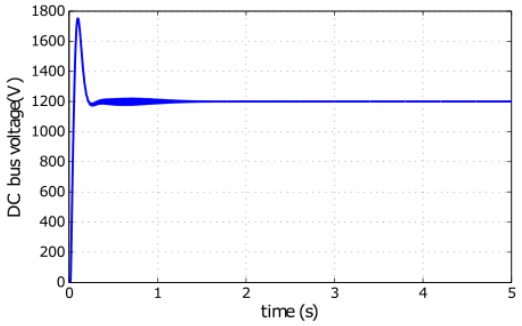

Fig. 20. DC bus voltage

Fig.15 illustrates the profile of the average wind speed used in simulation, while fig.16 shows the shaft rotational speed derived from the turbine. Fig.17 shows that the electromagnetic torque follows its reference, which allows for optimum power shown in fig.18, and we can see in fig.19 that the reactive power follows its reference exactly, this is due to control of direct and quadrature components of the rotor current. Finally, fig.20 shows that the DC bus voltage is perfectly regulated at 1200V.

7 Conclusion

This paper dealt with the modeling and control of a variable speed wind turbine system based on a DFIG. First, we explained why this wind system is the most widely used, partly because of savings from low sizing phase static converters implemented. Then we are interested in modeling the various constituents of the wind system. In fact, the aerodynamic and mechanical models of the turbine have been developed. Then, in order to establish the different commands of the two converters, we developed the model of DFIG. Finally, we implemented the vector control based on PI regulators. The results obtained demonstrate that the proposed control is effective and have many benefits.

References:

[1] T. Ackermann et L. Soder, «An overview of wind energy-status,» chez *Renewable and Sustainable Energy Reviews 6(1-2), 67-127*, 2002.

[2] T. Burton, D. Sharpe, N. Jenkins et E. Bossanyi, Wind Energy Handbook, John Wiley&Sons, Ltd,, 2001.

[3] W. L. Kling et J. G. Slootweg, Wind Turbines as Power Plants, Oslo, Norway: in Proceeding of the IEEE/Cigré workshop on Wind Power and the impacts on Power Systems, 17-18 June 2002.

[4] L. Xu et C. Wei, Torque and Reactive Power Control of a Doubly Fed Induction Machine by Position Sensorless Scheme, IEEE Trans, Industry Application, vol. 31, no. 3, pp. 636 - 642, May/June 1995.

[5] A. Alesina et M. Venturini, Intrinsic Amplitude Limits and Optimum Design of 9 Switches Direct PWM AC-AC converter, Proc. of PESC con. pp. 1284-1290, Rec, April 1988.

[6] D. Seyoum et C. Grantham, Terminal Voltage Control of a Wind Turbine Driven Isolated Induction Generator using Stator Oriented Field Control, IEEE Transactions on Industry Applications, pp. 846-852, September 2003.

[7] A. DAVIGNY, «Participation aux services système de fermes éoliennes à vitesse variable intégrant un stockage inertiel d'énergie,» Thèse de Doctorat, USTL Lille (France), 2007.

[8] K. GHEDAMSI, «Contribution à la modélisation et la commande d'un convertisseur direct de fréquence.Application à la conduite de la machine asynchrone,» Thèse de Doctorat, ENP Alger (Algérie), 2008.

[9] M. Budinger, D. Leray et Y. Deblezer, «Eoliennes et vitesse variable,» La revue 3EI, vol. 21, pp. 79-84, 2000.

[10] S. El Aimani, B. François, F. Minne et B. Robyns, «Comparison analysis of control structures for variable wind speed turbine,» chez *Proceedings of CESA*, Lille, France, Juillet 2003.

[11] B. Bossoufi, K. Mohammed, A. Lagrioui, M. Taoussi, and M. L.ElHafyani, "Backstepping control of dfig generators for wide-range variable-speed wind turbines," International Journal of Automation and Control, vol. 8, no. 2, pp. 122–140, 2014.

[12] E. Muljadi, «Pitch-controlled variable-speed wind turbine generation,» *IEEETransaction on Industry Applications,* vol. 37, n° %11, Jan./Feb 2001.

[13] S. E. Ben Elghali, «Modélisation et Commande d'une hydrolienne Equipée d'une génératrice Asynchrone Double Alimentation,» JGGE'08, 16-17, Lyon (France), Décembre 2008.

[14] S. El AIMANI, «Modélisation de différentes technologies d'éoliennes intégrées dans un réseau de moyenne tension,» Thèse de Doctorat, École Centrale de Lille (France), 2004.

[15] F. Poitiers, «Etude et commande de génératrices asynchrones pour l'utilisation de l'énergie éolienne,» Ecole Polytechnique de Nantes (France), 2003.

[16] M. C. Benhabib, «Contribution à l'étude des différentes topologies et commandes des filtres actifs parallèles à structure tension: modelisation,simulation et validation expérimentale de la commande,» Thèse de doctorat, Université Henri Poincaré, Nancy-Université, France, 2004.

[17] A. GAILLARD, «Système éolien basé sur une MADA : contribution à l'étude de la qualité de l'énergie électrique et de la,» Université Henri Poincaré, Nancy-I (France), 2010.